Proceedings of the 3rd IEEE Int. Conf. on
Nano/Micro Engineered and Molecular Systems
January 6-9, 2008, Sanya, China

Study on Multi-scale-Based 3-D Surface Topography Evaluation Algorithm

Jun Wang[1, 2, *], Yan Kang[3]

[1] *School of Mechanical Science & Engineering, Huazhong University of Science and Technology, China*
[2] *College of Mechatronics Engineering, China Jiliang University, China*
[3] *Youse Mapping &Conveying Institute of Zhejiang, China*

***Abstract*—In machining and testing field of MEMS parts, due to anisotropy commonly exists in some technics, the evaluation for 3-D surface topography is a difficult program. Existing evaluation algorithm is short of representation capability.**

Based on discussing of extracting methods of surface topography characteristics, the contourlet Transform (CT) which may provide tight bracing and mutli-scale analysis was introduced. We present a new 3-D surface topography evaluation algorithm. This algorithm has some excellent performances such as multi-scale analysis, high-resolution, time-frequency-localization and multi-directions. And it is good at describing high dimensions data. Meanwhile, according to the theory that noise is not correlated with signal, correlation theory was explored as Discriminant Function. The contourlet transform is rebuilt to an adaptive filter based on this discriminant. Thus high-frequency noise, roughness and waviness information may be separated from. However, we found a question in experiment, so a datum plane was established according to the definition of flatness. Above-mentioned CT and two discriminants may be seen as three low-pass filter banks from the view of filtering. Thus, microcosmical 3-D surface topography of a part may be appraised finely under the three filters work together.

The algorithm is verified by simulations. A conclusion can be draw that this algorithm can reliably obtain benchmark of appraisemnt. And the surface information of measured part can be extracted and analyzed without distortion. Comparing with existent 3-D surface topography evaluation algorithm, this method is preponderant in practicality of MEMS and nano surface evaluation.

Keywords- correlation; contourlet tansform; MEMS; surface topography

I. INTRODUCTION

Now, ultra-precision machining and nanofabrication is regarded as important technologies by researchers of the world. So do the testing technologies of surface topography.

Development of Sub-micron and nanofabrication technology, such as Líthographíe, Galvanoformung, Abformung (LIGA), coating, splashing and probe etc., is so quickly that the manufactured or processed surface may arrive at nano-scale. Meanwhile, with the appearance of scanning tunneling microscope (STM), X-ray Nano-scale Interferometry and laser Interferometry, description for atomic structure of microcosmic surface come to possible. Manufacture methods and measurement technologies continuously improve and walk to factory from laboratory too; however, the evaluation system, measurement strategy and term describing these performances have not almost changed during this period. Nevertheless, some scholars still actively explore and study the surface topography of ultra-precision machining and nanofabrication [1-5].

The surface topography is an important factor influencing part performances (such as friction, abrasion, lubrication, coating and painting etc.). In machining part, different feature would come into being according to relevant machining techniques (for example turning, milling and grinding). The variation of machining condition will influence the variation of surface topography. Thus, if the topography of machined surface is decomposed to different space and frequency bands and these decompositions can be corresponded with the variation of a certain machining process. A testing technique will be developed to monitor machining process by analyzing variation of surface topography. The preconditions of building this relationship are: to extract different surface features correctly; to create an effective analysis method for these features, i.e., to establish the relation between the variation of the surface features and the variation of machining conditions [6].

Accurately extracting surface features are greatly useful for appraising surface function and enhancing part performance. They include extracting not only roughness, waviness and form of separated surface but also multi-scale topography features (the peaks/pits and ridges/valleys) without aliasing along the edges of these features [7]. Further more, along with the developing of science and technology, the demand for surface quality has been enhanced to nanometer scale, even to atom scale. Surface measurement technology has been developed to 2-D surface from 1-D profile. The surface of nanometer scale contains more abundant and finer information than traditional one. Accordingly, more advanced surface analysis technologies and methods are demanded to accurately extract useful information from these measured surfaces. The traditional surface feature extraction focuses on surface roughness analysis where midline evaluation benchmark and filtering are used for long time. The midline evaluation benchmarks mainly include Least Square Regression midline and Arithmetic

This project was funded by National Natural Science Foundation of China (Project code: 50175037) and Science and Technology Department of Zhejiang Province (Project code: 2006c21127).

*Contact author: ***blackknight@cjlu.edu.cn***

Average midline as well as Polynomial fit midline. The filters include 2RC filter, spline filter, Gaussian filter, Gaussian regression filter and Gaussian robust filter derived from Guassian filter [8]. The evaluation of surface function features requires 3-D analysis and evaluation. The multiscale analysis technique was introduced along with the development of space surface feature evaluation. Meanwhile, MOTIF based on surface morphology has made a great progress too. It has been extensively applied at surface evaluation of car's armor plate and makes success in evaluation of MEMS parts.

By dynamical changing the size of frequency window in analysis, the wavelet analysis provides space and time locating capability which can not been provided from base function derived from sine signal or pulse function. Nevertheless, in 2-D and 3-D data processing, wavelet analysis meets difficulty too. The cause is that wavelet is decomposed just in horizontal and vertical direction. And in higher dimension information, direction of the useful data is complicated. Thus, the efficiency and veracity of wavelet analysis is damaged. In order to solving this problem, many new methods are put forward.

In recent years, the evaluation method of surface analysis has been greatly developed. The ameliorated space surface evaluation method provided possibility for dynamical monitoring surface machining process and further function evaluation. In this paper, on the basis of recent development of signal processing technology, we further explore multi-scale analysis method of surface topology based on CT. The CT and correlation theories are introduced into the areas of surface analysis in this study. As a result, the inherent shortcoming of traditional analysis method is solved and exactly extraction on surface features is realized.

II. CONTOURLET TRANSFORM

A. Comparing with Wavelet Transform

Wavelet transform (WT) would take many wavelet coefficients to accurately represent even one simple 2-D curve, so CT were developed as an improvement over WT in terms of this inefficiency. The CT has the multi-scale and time-frequency-localization properties of WT; meanwhile it offers a high degree of directionality and anisotropy. Precisely, CT involves basis functions that are oriented at any power of two's number of directions with flexible aspect ratios. With such richness in the choice of basis functions, CT can represent any 1-D smooth edges with close to optimal efficiency. Fig. 1 shows that compared with WT, CT can represent a smooth contour with much fewer coefficients [9].

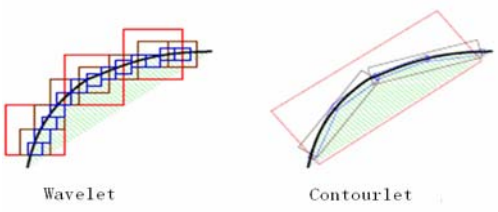

Figure 1. Wavelet versus Contourlet: illustrating the successive refinement by the two systems, where Contourlet using fewer coefficients than wavelet.

B. Pyramidal directional filter bank and iterated directional filter banks

Contourlets are implemented by the pyramidal directional filter bank (PDFB) that is a cascade of a laplacian pyramid (LP) and a directional filter bank (DFB) [10]. Due to this cascade structure, multiscale and directional decomposition stages in the CT are independent of each other. We can decompose each scale into any arbitrary power of two's number of directions, and different scales can be decomposed into different numbers of directions.

Bamberger and Smith [11] constructed a 2-D directional filter bank (DFB) that can be maximally decimated while achieving perfect reconstruction. To obtain the desired frequency partition, a complicated tree expanding rule has to be followed for finer directional subbands [12]. In [13], a new construction was proposed for the DFB that avoids modulating the input image and has a simpler rule for expanding the decomposition tree. This DFB is intuitively constructed from two building blocks. The first building block is a two-channel quincunx filter bank [14] with fan filters (see Fig. 2) that divides a 2-D spectrum into two directions: horizontal and vertical. The second building block of the DFB is a shearing operator, which amounts to just reordering of image samples.

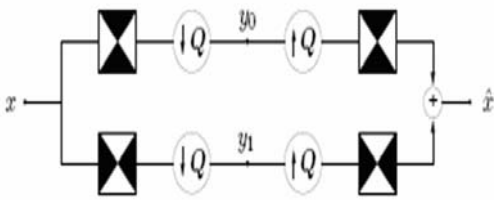

Figure 2. Frequency partition using quincunx filter banks with fan filters. The black regions represent the ideal frequency supports of each filter. Q is a quincunx sampling matrix.

III. BUILDING DISCRIMINANT FOR FILTERING

A. Correlation Theory

Essentially, CT filters noise from signal by means of limited iterative decompositions and reconstructions. But the levels of decomposition and the threshold value of reconstruction is very dependent on individual experience. Therefore, there is strongly subjectivity when the data is processed. According to relational theories of that signal is not correlated with noise, an objective filtering rule is proposed in this paper. Generally, the signals containing noise are processed as Fig. 3.

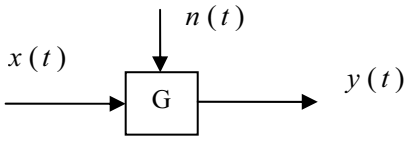

Figure 3. Signals flow chart. Where $x(t)$ is input signals, $n(t)$ is noise, G represents processing system and $y(t)$ is output signals.

Thus, the cross correlation function of input signals and output signals is:

$$r_{xy}(t) = \int_{-\infty}^{+\infty} [x(t) + n(t)] * y(t-\tau)dt \tag{1}$$

Unwrapping (1), the cross correlation function may be written as following:

$$r_{xy}(t) = \int_{-\infty}^{+\infty} x(t) * y(t-\tau)dt + \int_{-\infty}^{+\infty} n(t) * y(t-\tau)dt \tag{2}$$

The autocorrelation function of output signals is:

$$r_{y^2}(t) = \int_{-\infty}^{+\infty} y(t) * y(t-\tau)dt \tag{3}$$

In the ideal case that noise may be fully filtered out and the direct current part of both signal and noise are also taken out, the first part of the (2) is an autocorrelation function of output signals, and the second part is zero. The difference between (1) and (2) is described with e (t), thus,

$$\begin{aligned} e(t) = r_{xy}(t) - r_{y^2}(t) = \int_{-\infty}^{+\infty} x(t) * y(t-\tau)dt + \\ \int_{-\infty}^{+\infty} n(t) * y(t-\tau)dt - \int_{-\infty}^{+\infty} y(t) * y(t-\tau)dt = 0 \end{aligned} \tag{4}$$

Based on above-mentioned expressions, the levels of decomposition and reconstruction may be controlled; consequently, noise may be filtered from signal according to our requirement

Furthermore, the information contained in surface topography may be classified into form information, waviness information and surface roughness information. We supposed that noise has been filtered; the information may be fractionized as:

$$x(t) = x_1(t) + x_2(t) \tag{5}$$

where $x_1(t)$ represents waviness information and $x_2(t)$ represents roughness information. The new information flow may be described as Fig. 4.

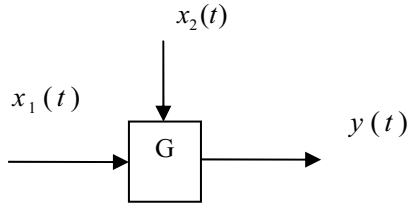

Figure 4. Signals flow chart. Where $x_1(t)$ is waviness signals, $x_2(t)$ is roughness signals, G represents processing system and $y(t)$ is output signals.

Similarly, we still describe cross correlation function of input signals and output signals with $R_{xy}(t)$; and described autocorrelation function of output signals with $R_{y^2}(t)$. Consequently,

$$R_{xy}(t) = \int_{-\infty}^{+\infty} [x_1(t) + x_2(t)] * y(t-\tau)dt \tag{6}$$

$$R_{y^2}(t) = \int_{-\infty}^{+\infty} y(t) * y(t-\tau)dt \tag{7}$$

$E(t)$ is used to describe the difference between (6) and (7). We get:

$$\begin{aligned} E(t) &= R_{xy}(t) - R_{y^2}(t) \\ &= \int_{-\infty}^{+\infty} [x_1(t) + x_2(t)] * y(t-\tau)dt - \int_{-\infty}^{+\infty} y(t) * y(t-\tau)dt \end{aligned} \tag{8}$$

Under ideal case, the roughness information $x_2(t)$ has been fully filtered out. $y(t) = x_1(t)$. Thus, an expression may be obtained by cleaning up the (8).

$$E(t) = R_{xy}(t) - R_{y^2}(t) = \int_{-\infty}^{+\infty} x_2(t) * y(t-\tau)dt \tag{9}$$

It can be estimated by relative definition about waviness and roughness. Therefore, the waviness information and roughness information may be distinguished with.

B. Flatness Discriminant

Theoretically, the part-measured reference flat can be obtained by continually filtering. However, the experimental results do not support this guess. The reasons leaded this result maybe improper configuration for filters, improper choice for iterative discriminant function or else unknown factors. In order to solve this problem, according to the definition of flatness, we use part-measured Least-squares flat simulating reference flat. The idiographic method is as below:

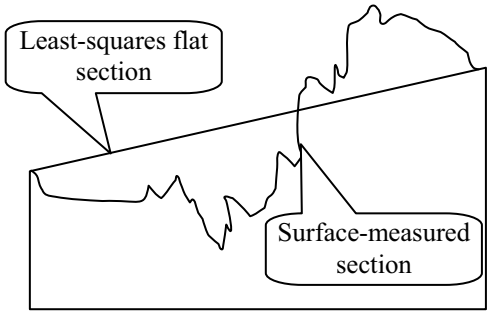

Figure 5. The schematic chart of reference flatness and waviness

Supposed least-square flat is:

$$z = ax + by + c \tag{10}$$

And Q is sum of the square lengths from surface-measured to counterpart point of Least-square flat, then:

$$Q = \sum_{i=1}^{m \times n} (z_i - ax_i - by_i - c)^2 \tag{11}$$

By ordering $\frac{\partial Q}{\partial a} = 0$, $\frac{\partial Q}{\partial b} = 0$ and $\frac{\partial Q}{\partial c} = 0$, we may solve *minQ*. The flat made certain with parameters-solved *a, b* and *c* is just

the least-square flat. With $\frac{\partial Q}{\partial a}=0$, $\frac{\partial Q}{\partial b}=0$ and $\frac{\partial Q}{\partial c}=0$, three equations are respectively obtained as following:

$$\sum_{i=1}^{m\times n} 2x_i(z_i - ax_i - by_i - c) = 0 \tag{12}$$

$$\sum_{i=1}^{m\times n} 2y_i(z_i - ax_i - by_i - c) = 0 \tag{13}$$

$$\sum_{i=1}^{m\times n} 2(z_i - ax_i - by_i - c) = 0 \tag{14}$$

By coordinating above-mentioned three equations, we get a new equation array:

$$\begin{cases} a\sum_{i=1}^{m\times n} x_i^2 + b\sum_{i=1}^{m\times n} x_i y_i + c\sum_{i=1}^{m\times n} x_i = \sum_{i=1}^{m\times n} x_i z_i \\ a\sum_{i=1}^{m\times n} x_i y_i + b\sum_{i=1}^{m\times n} y_i^2 + c\sum_{i=1}^{m\times n} y_i = \sum_{i=1}^{m\times n} y_i z_i \\ a\sum_{i=1}^{m\times n} x_i + b\sum_{i=1}^{m\times n} y_i + c\sum_{i=1}^{m\times n} 1 = \sum_{i=1}^{m\times n} z_i \end{cases} \tag{15}$$

And by using Cramer rule, we get the answers of the equations as following:

$$a = \begin{vmatrix} \sum_{i=1}^{m\times n} x_i z_i & \sum_{i=1}^{m\times n} x_i y_i & \sum_{i=1}^{m\times n} x_i \\ \sum_{i=1}^{m\times n} y_i z_i & \sum_{i=1}^{m\times n} y_i^2 & \sum_{i=1}^{m\times n} y_i \\ \sum_{i=1}^{m\times n} z_i & \sum_{i=1}^{m\times n} y_i & \sum_{i=1}^{m\times n} 1 \end{vmatrix} \Big/ \begin{vmatrix} \sum_{i=1}^{m\times n} x_i^2 & \sum_{i=1}^{m\times n} x_i y_i & \sum_{i=1}^{m\times n} x_i \\ \sum_{i=1}^{m\times n} x_i y_i & \sum_{i=1}^{m\times n} y_i^2 & \sum_{i=1}^{m\times n} y_i \\ \sum_{i=1}^{m\times n} x_i & \sum_{i=1}^{m\times n} y_i & \sum_{i=1}^{m\times n} 1 \end{vmatrix} \tag{16}$$

$$b = \begin{vmatrix} \sum_{i=1}^{m\times n} x_i^2 & \sum_{i=1}^{m\times n} x_i z_i & \sum_{i=1}^{m\times n} x_i \\ \sum_{i=1}^{m\times n} x_i y_i & \sum_{i=1}^{m\times n} y_i z_i & \sum_{i=1}^{m\times n} y_i \\ \sum_{i=1}^{m\times n} x_i & \sum_{i=1}^{m\times n} z_i & \sum_{i=1}^{m\times n} 1 \end{vmatrix} \Big/ \begin{vmatrix} \sum_{i=1}^{m\times n} x_i^2 & \sum_{i=1}^{m\times n} x_i y_i & \sum_{i=1}^{m\times n} x_i \\ \sum_{i=1}^{m\times n} x_i y_i & \sum_{i=1}^{m\times n} y_i^2 & \sum_{i=1}^{m\times n} y_i \\ \sum_{i=1}^{m\times n} x_i & \sum_{i=1}^{m\times n} y_i & \sum_{i=1}^{m\times n} 1 \end{vmatrix} \tag{17}$$

$$c = \begin{vmatrix} \sum_{i=1}^{m\times n} x_i^2 & \sum_{i=1}^{m\times n} x_i y_i & \sum_{i=1}^{m\times n} x_i z_i \\ \sum_{i=1}^{m\times n} x_i y_i & \sum_{i=1}^{m\times n} y_i^2 & \sum_{i=1}^{m\times n} y_i z_i \\ \sum_{i=1}^{m\times n} x_i & \sum_{i=1}^{m\times n} y_i & \sum_{i=1}^{m\times n} z_i \end{vmatrix} \Big/ \begin{vmatrix} \sum_{i=1}^{m\times n} x_i^2 & \sum_{i=1}^{m\times n} x_i y_i & \sum_{i=1}^{m\times n} x_i \\ \sum_{i=1}^{m\times n} x_i y_i & \sum_{i=1}^{m\times n} y_i^2 & \sum_{i=1}^{m\times n} y_i \\ \sum_{i=1}^{m\times n} x_i & \sum_{i=1}^{m\times n} y_i & \sum_{i=1}^{m\times n} 1 \end{vmatrix} \tag{18}$$

IV. EXPERIMENT AND ANALYSES

Two experiments have been done in this study. In experiment 1, we compared CT with WT in their filtering performance. The result shows that the CT takes advantages to the WT in 2-D information processing. In experiment 2, the STABCC filter structured by contourlet filters and correlation functions was used to processing 3-D surface profile information. And the result showed that CT is better than WT, but it didn't represent good enough in the edges.

A. Experimental 1: SNR Comparision between WT and CT

On the basis of contourlet box provided by Minh. N.DO, we rewrote some codes and processed a 512*512 gray-scale image 'Lena'. The result is shown as following:

Figure 6. 2-D image processing effect contrast, CT versus WT.

B. Experimental 2: Testing for 3-D Surface Topography

A surface-complicated 3-D topography is planned with MATLAB. And a simulation is conducted to verify aove-mentioned theories. The simulation result is illustrated as following:

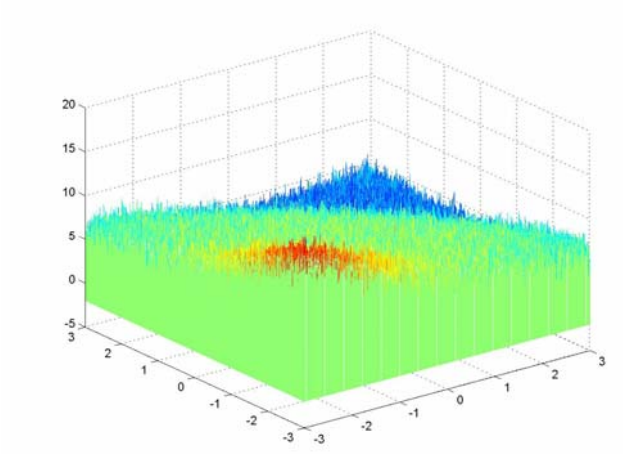

Figure 7. The original 3-D image containing noise, roughness, waviness and form information.

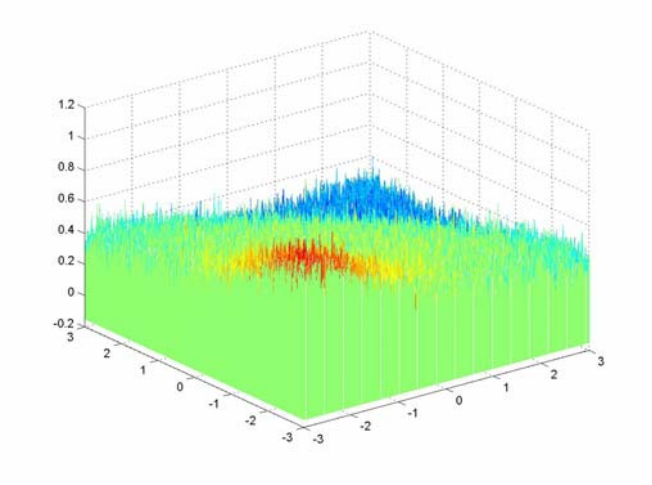

Figure 8. 3-D image processed with WT.

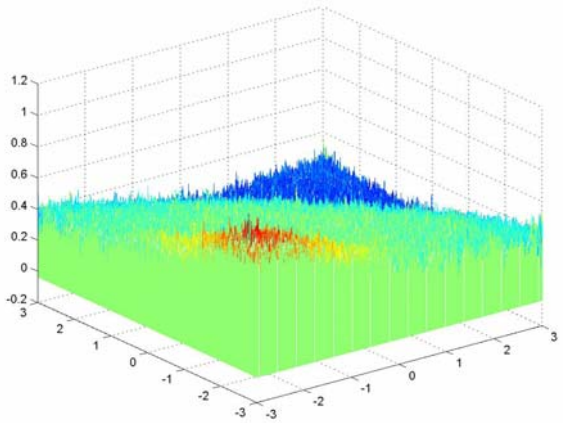

Figure 9. 3-D image processed with CT

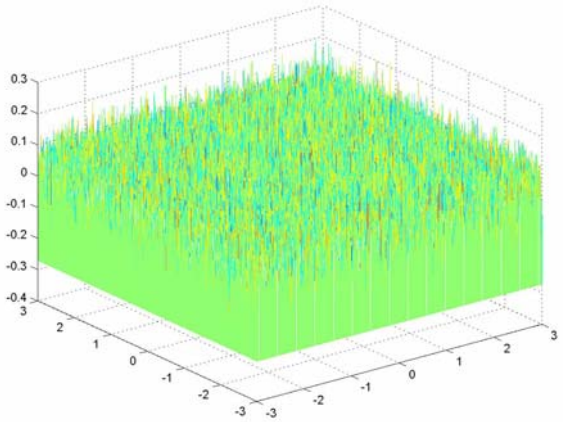

Figure 10. noise mage processed with WT.

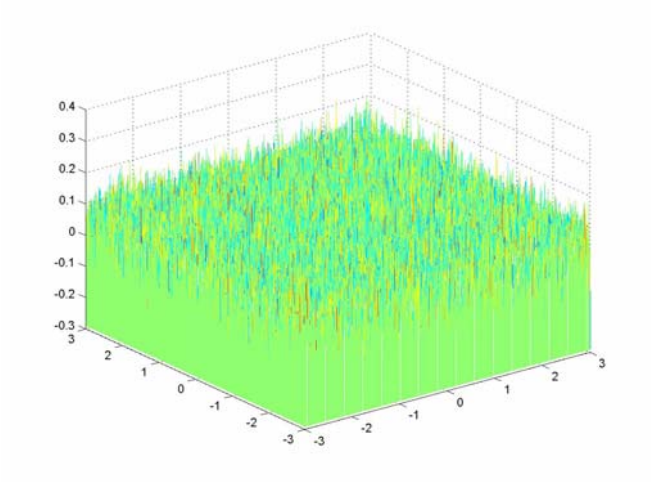

Figure 11. 3-D image processed with CT. It contains noise and roughness information.

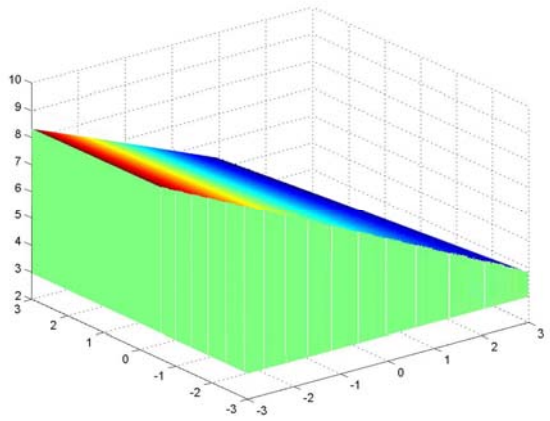

Figure 12. Least-square reference flat

V. CONCLUSION AND FUTURE WORKS

The results of the experiment 1 show that contourlet filtering is better than 2-D wavelet filtering in processing 2-D data. And the effect is expected well on condition that the algorithm is optimized. According to experiment 2, a conclusion can be draw that contourlet filtering represents outstanding performance in 3-D data processing. Combined with correlation theories and flatness discriminant, contourlet filtering can be rebuilt into an adaptive filter array. Its shortcoming is distortion produced on edges. We will focus on it in further work.

ACKNOWLEDGMENT

The authors would like to thank Dr. Y. T. Li for the fruitful discussions.

REFERENCES

[1] T. Ahbe, N. Haft, K. Hasche, and K. P. Hoffmann, "Geometrical measurements on film structures using a scanning electron microscope," in: Micro System Technologies 98, Sixth International Conference on Micro Electro, Opto, Mechanical Systems and Components, PotsdamyGermany, December, 1998, pp. 627–629.

[2] A. Stesmans, K. Clémer, and V.V. Afanas'ev, "The E_{γ}' center as a probe of structural properties of nanometer-sized silica particles," Non-Crystalline Solids, Leuven, Belgium, xxx (2007) xxx–xxx.

[3] Junsok Lee, and Soohyun Kim, "Manufacture of a nanotweezer using a length controlled CNT arm, " Sensors and Actuators , vol. A 120, 2005, pp. 193–198.

[4] K.-P. Hoffmann, T. Ahbe, K. Herrmann, K. Hasche, F. Pohlenz, and J. Sun, "Development and calibration of standards for the coating thickness in the range of micrometer and nanometer," Surface and Coatings Technology, vol. 169 –170, 2003, pp. 732–734.

[5] Hae-Sung Kim, Tae-Youb Kimb, Yark-Yeon Kimb, Gee-Pyeong Hanb, b a a Mun-Cheol Paek , Dong-Hoon Shin , and Jin-Koo Rhee, "F abrication technology for improving pattern quality in focusing waveguide grating coupler manufacture," Microelectronic Engineering, vol. 65, 2003, pp. 307–318.

[6] Q. H. Chen, "Surface roughness evaluation by using wavelets analysis," Precision Engineering, vol. 23(3), 1999, pp. 209-212.

[7] M. Krystek, "A fast Gauss filtering algorithm for roughness measurements," Precision Engineering, vol. 19(2), 1996, pp. 198 – 200.

[8] W. Zeng, X. Jiang, and P. Scott, "Metrological Characteristics of Dual Tree Complex Wavelet Transform for Surface Analysis," Measurement Science and Technology, vol. 29(7), 2002, pp. 125 – 131.

[9] D. L. Donoho, M. Vetterli, R. A. DeVore, and I. Daubechies, "Data compression and harmonic analysis," IEEE Trans. Inform. Th, vol. 44(6), 1998, pp. 2435–2476.

[10] A. Skodras, C. Christopoulos, and T. Ebrahimi, "The JPEG 2000 still image compression standard," IEEE Signal Processing Magazine, vol. 18, 2001, pp. 36–58.

[11] E. J. Cand`es and D. L. Donoho, "Curvelets – a surprisingly effective nonadaptive representation for objects with edges," Curve and Surface Fitting, vol. 28(5), 2001, pp. 36–58.

[12] D. H. Hubel and T. N. Wiesel, "Receptive fields, binocular interaction and functional architecture in the cat's visual cortex," Journal of Physiology, vol. 160, 1962, pp. 106–154.

[13] B. A. Olshausen and D. J. Field, "Emergence of simple-cell receptive field properties by learning a sparse code for natural images," Nature, 1996, pp. 607–609.

[14] E. J. Candès and D. L. Donoho, "Ridgelets: a key to higher-dimensional intermittency?" Phil. Trans, 1999, pp.2495–2509.